Journal of Thermal Analysis and Calorimetry, Vol. 66 (2001) 409–414

LOW TEMPERATURE SPECIFIC HEAT AND THERMAL STABILITY OF Fe–B ULTRAFINE AMORPHOUS ALLOY PARTICLES

L. Wang[1], *Z. C. Tan*[1*], *S. H. Meng*[1], *D. B. Liang*[2], *S. J. Ji*[3] *and Z. K. Hei*[3]

[1]Thermochemistry Laboratory, Dalian Institute of Chemical Physics, Chinese Academy of Sciences, Dalian 116023, China
[2]Environmental Engineering Laboratory, Dalian Institute of Chemical Physics, Chinese Academy of Sciences, Dalian 116023, China
[3]Institute of Material and Technology, Dalian Maritime University, Dalian 116026, China

(Received December 14, 2000; in revised form April 30, 2001)

Abstract

Fe–B ultrafine amorphous alloy particles (UFAAP) were prepared by chemical reduction of Fe^{3+} with $NaBHO_4$ and confirmed to be ultrafine amorphous particles by transmission electron microscopy and X-ray diffraction. The specific heat of the sample was measured by a high precision adiabatic calorimeter, and a differential scanning calorimeter was used for thermal stability analysis. A topological structure of Fe–B atoms is proposed to explain two crystallization peaks and a melting peak observed at T=600, 868 and 1645 K, respectively.

Keywords: DSC, Fe–B amorphous alloy, specific heat, thermal stability, ultrafine particle

Introduction

Fe–B amorphous alloys are used as catalysts for many chemical reactions and have been found to be active and selective for the hydrogenation of olefins and organic functional groups [1, 2]. Furthermore, they can be used as ferrofluids and magnetic recording materials [3]. Many studies have focused on the preparation and characterization of Fe–B ultrafine amorphous alloy particles (UFAAP) produced by the reduction of metal salts with borohydride in an aqueous solution [4–6]. However, little attention has been devoted to the thermodynamic properties of Fe–B UFAAP. Due to the ultrafine grain size, there are a great number of grain boundaries which make up as much as 50 vol% in a 5 nm nanocrystalline material [7], and the heat capacity of nanocrystalline Pd with particle size of 6 nm increases 55% compared to the coarse crystalline Pd [8]. The sintering temperature of ultrafine particles is also much lower than that of the coarse particles, for example, nanocrystalline Al_2O_3 can be sintered at

* Author to whom all correspondence should be addressed. E-mail: tzc@ms.dicp.ac.cn; Fax: 86-411-4691570

1418–2874/2001/ $ 5.00

Akadémiai Kiadó, Budapest
Kluwer Academic Publishers, Dordrecht

a temperature of 1423 K, while the normal one can only be sintered at temperature of 2073–2173 K [9]. Since Fe–B UFAAP has wide fields of application, and ultrafine particles may exhibit novel and improved properties, it is of interest to investigate their thermodynamic properties.

This paper reports a first attempt to measure the low temperature specific heat of Fe–B UFAAP as well as the thermal stability associated with applications of the material.

Experimental

Sample preparation and chemical analysis

Fe–B UFAAP sample was prepared by adding 6.6255 g $NaBH_4$ powder slowly into 500 mL 0.3 mol L^{-1} $FeCl_3$ solution under vigorous stirring for 2 h at room temperature. The black precipitate was washed thoroughly with distilled water in order to remove residual ions from the reaction mixture, and followed by washing with acetone for drying.

The chemical composition of the prepared sample was determined by chemical analysis with dimethylglycine and ethylenedinitrilotetra-acetic acid (EDTA) which has been reported previously in detail [4].

Sample characterization

A Shimadzu X-ray diffractometer (XRD-6000) with CuK_α radiation was used for X-ray diffraction to identify the structure of the sample. The morphology and particle size of the sample was determined by a transmission electron microscopy (TEM, Philips-EM420). The sample was dispersed by ultrasonic vibrations, and ethanol was used as dispersant.

Specific heat measurement

The specific heat of the sample at low temperature was measured with an adiabatic calorimeter with the volume of 6 cm^3 for small samples. The construction of the calorimeter has been described in detail elsewhere [10]. Briefly, the construction of the calorimeter included a sample cell, a thermometer, a heater, two adiabatic shields, two sets of 8-junction chromel-copel thermocouples, and a high vacuum system. The calorimeter cell was made of gold-plated copper with internal capacity of 6 cm^3. A miniature platinum resistance thermometer made by Shanghai Institute of Industrial Automatic Meters, China, was used to measure the temperature of the calorimeter cell. The thermometer with an uncertainty of about 1 mK (in absolute) was calibrated on the basis of ITS-90 by the station of low temperature metrology, Chinese Academy of Sciences. The thermometer was placed in the copper sheath at the bottom of sample cell. After loading the sample into the cell, the up-cover and body were sealed with a special kind of cycleweld. The cell was evacuated, and then a small amount of helium gas was introduced through a copper capillary on the up-cover to promote the heat transfer. Finally, the cell was sealed by pinching off the tube. Two adiabatic shields surrounded the cell and controlled its temperature. The whole calorimetric

system was kept in a high vacuum with residual pressure of 10^{-3} Pa to obtain good adiabatic conditions. In order to verify the reliability of the calorimeter, the molar heat capacity of α-Al_2O_3 were measured in the temperature range of 60–350 K. Deviations of the experimental results from the smoothed curve lie within ±0.2%, and the inaccuracy is within ±0.5%, as compared with those of the National Bureau of Standards [11] over the investigated temperature range. The mass of the Fe–B UFAAP sample used for the adiabatic calorimetric study is 2.3622 g.

Thermal analysis

The thermal stability analysis was performed by a differential scanning calorimeter (DSC, Netzsch 409). Pure argon (99.999%) was used for purging the sample holders in the DSC. An Al_2O_3 pan was used as sample container and an empty Al_2O_3 pan served as the reference material. The sample of about 10 mg was measured with a heating rate of 10 K min^{-1}.

Results and discussion

Composition, structure and grain size

Chemical analysis showed that the fraction of Fe and B are 52 and 48% in mass, respectively. XRD measurement revealed that the sample is a typical amorphous substance, as no sharp crystalline reflections were observed. Transmission electron micrograph (TEM) indicated that the reaction product consists of highly dispersed nanometer sized particles with uniform shape. The average diameter of the particles measured by TEM is 31 nm and the distribution of the diameters conforms to a Boltzmann distribution.

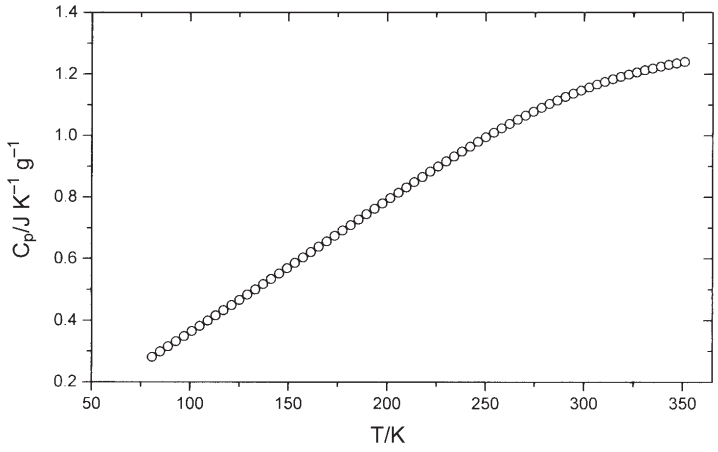

Fig. 1 Specific heat of Fe–B UFAAP as a function of temperature

Specific heat

The experimental data of specific heat for the Fe–B UFAAP are listed in Table 1 and plotted in Fig. 1. The temperature dependence of specific heat for 80–350 K can be described by the following relations:

$$C_p(\mathrm{J\ g^{-1}\ K^{-1}}) = -0.34194 + 0.01342T - 1.22630\cdot10^{-4} + 6.34782\cdot10^{-7}T^3 + \\ + 1.64834\cdot10^{-9}T^4 + 1.55683\cdot10^{-12}T^5$$

in which T represents the measurement temperature.

Table 1 Experimental specific heat of Fe–B UFAAP ($Fe_{52}B_{58}$ in mass)

T/K	C_p/J g^{-1} K^{-1}	T/K	C_p/J g^{-1} K^{-1}	T/K	C_p/J g^{-1} K^{-1}
83.142	0.2846	165.937	0.6314	244.470	0.9891
86.223	0.3008	169.004	0.6463	247.859	1.0090
89.194	0.3130	172.034	0.6580	251.217	1.0160
92.072	0.3255	175.031	0.6741	255.503	1.0206
94.865	0.3391	177.992	0.6880	260.132	1.0312
97.585	0.3512	180.921	0.7016	261.170	1.0384
100.239	0.3678	183.820	0.7152	263.624	1.0417
103.056	0.3810	186.687	0.7286	267.588	1.0467
106.026	0.3904	189.529	0.7421	271.018	1.0491
108.924	0.4024	192.337	0.7615	274.283	1.0557
112.022	0.4191	195.118	0.7678	277.527	1.0679
115.316	0.4319	197.879	0.7845	280.859	1.0749
118.538	0.4466	200.617	0.7965	284.371	1.0796
121.695	0.4589	203.472	0.8044	288.047	1.0896
124.795	0.4694	206.445	0.8174	292.657	1.1044
127.841	0.4818	209.400	0.8352	296.385	1.1204
130.836	0.4924	212.336	0.8500	299.957	1.1612
133.789	0.5022	215.245	0.8591	304.741	1.1886
136.699	0.5185	218.145	0.8697	308.470	1.1991
139.86	0.5344	220.982	0.8803	312.339	1.2030
143.269	0.5454	223.818	0.9009	316.681	1.2071
146.628	0.5559	226.635	0.9111	321.081	1.2158
149.945	0.5692	230.434	0.9158	326.082	1.2198
153.234	0.5713	232.223	0.9340	330.711	1.2253
156.483	0.5872	235.148	0.9525	336.303	1.2325
159.677	0.6048	237.826	0.9735	342.796	1.2361
162.828	0.6210	240.655	0.9851	348.388	1.2368

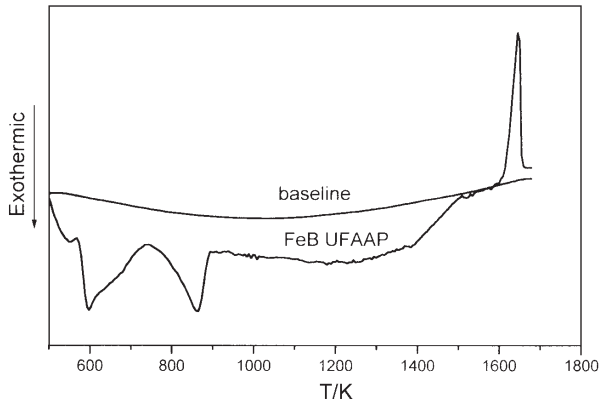

Fig. 2 Differential scanning calorimetric curve of the Fe–B UFAAP

The specific heat curve of the sample rises with increasing temperature in a smooth and continuous mode, indicating that no phase transition and thermal anomaly have taken place over this temperature range.

Thermal stability

Differential scanning calorimetry (DSC) was carried out to characterize the crystallization temperature and thermal stability of the Fe–B UFAAP. As shown in Fig. 2, two exothermic peaks and one endothermic peak were observed at 600, 868 and 1645 K respectively. Obviously, the endothermic peak is responsible for melting and the two exothermic peaks should be corresponding to crystallization. To explain the crystallization process, a topological structure of the atoms in the Fe–B UFAAP sample is suggested similarly to that proposed by Shen *et al*. in a Ni–P–B UFAAP system

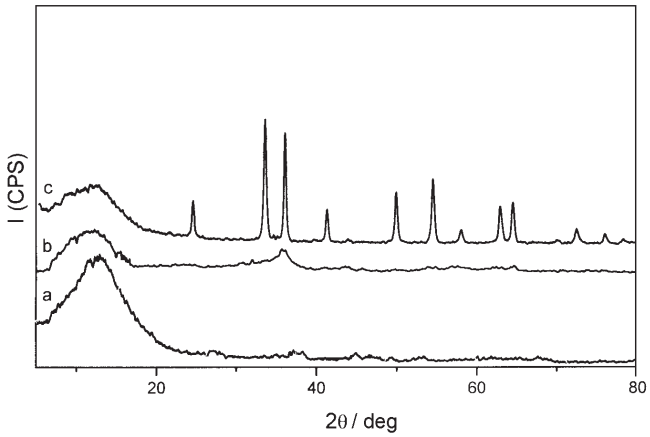

Fig. 3 X-ray diffraction patterns for Fe–B UFAAP annealed in Ar at the following different temperatures: a – as-prepared; b – 600 K; c – 868 K

[12]. According to this mode, the metalloid element B in the sample is not homogeneously distributed. The iron atoms with fewer nearest-neighbor metalloid atoms crystallize first. The iron atoms richer in metalloid neighbors are relatively stable and crystallize only at high temperatures with the formation of iron boride. This suggestion has been proved by further XRD experiments.

XRD pattern of amorphous Fe–B UFAAP and samples annealed at T=600 and 868 K for 1 h in pure argon atmosphere was shown in Fig. 3. Figure 3 (b) indicates that heat treatment at 600 K leads mainly to the formation of crystalline iron metal, which evidenced by the α-Fe_2O_3 (110) peak, because Fe–FeO oxygen partial pressure is quite low and thus was oxidized by trance oxygen in argon. Further heat treatment at 868 K suggests that the other peaks appearing in Fig. 3 (c) can be assigned to the crystalline phase of iron boride [13].

It is worth pointing out that Fe–B UFAAP are good catalysts, while no catalytic activities have been observed for Fe–B crystals. Accordingly, it is reasonable to conclude that the upper limit of effective temperature is 600 K for Fe–B to be used as catalyst.

* * *

This work is financially supported by the National Natural Science Foundation of China under Grant No. 20073047.

References

1 C. A. Brown and H. C. Brown, J. Am. Chem. Soc., 85 (1963) 1003.
2 P. Duwez, R.H. Willens and W. J. Jr. Kelement, Appl. Phys., 31 (1960) 1136.
3 S. Linderoth and S. Morup, J. Appl. Phys., 67 (1990) 4472.
4 T. X. Li, X. F. Zhang and C. D. Jin, Chin. J. Catal., 6 (1995) 299.
5 A. Martino, M. Atoker, M. Hicks, C. H. Bartholomew, A. G. Sanlt and J. S. Kawola, Appl. Catal., A: General, 161 (1997) 235.
6 J. Y. Sun, Z. Y. Li, Q. G. Wang and Y. Chen, J. Mater. Sci., 32 (1997) 749.
7 X. Zhu, R. Birringer, U. Herr and H. Gleiter, Phys. Rev. B, 35 (1987) 9085.
8 J. Rupp and R. Birrnger, Phys. Rev. B, 36 (1987) 7888.
9 T. S. Yeh and M. D. Sacks, J. Am. Ceram. Soc., 71 (1988) 841.
10 Z. C. Tan, G. Y. Sun and Y. Sun, J. Thermal Anal., 45 (1995) 59.
11 D. A. Ditmarts, S. Ishihara, S. S. Chang, G. Bernstchin and E. D. West, J. Res. Nat. Bur. Stand., 87 (1982) 159.
12 J. Y. Shen, Z. Hu, Q. H. Zhang, L. F. Zhang and Y. Chen, J. Appl. Phys., 71 (1992) 5217.
13 Joint Committee on Powder Diffraction Standards – International Center for Diffraction Data, PCPDFwin Version 1.30, 1997.